Improving Performance of Polarizable Continuum Model for Study of Large Molecules in Solution

NADIA REGA, MAURIZIO COSSI, VINCENZO BARONE

Dipartimento di Chimica, Università Federico II, Via Mezzocannone 4, I-80134 Napoli, Italy

Received 4 January 1999; accepted 30 March 1999

ABSTRACT: We present a new implementation of the polarizable continuum model (PCM) that significantly improves its performance, especially for large solutes. This approach avoids the separation between electronic and nuclear sources in the calculation of the solvation charges, allowing the extension of iterative procedures to all the PCM versions [dielectric (D), conductor (C), and integral equation formalism (IEF)], so that the best method and/or algorithm can be selected, depending on the system at hand. In particular, the new balanced two-term iterative procedure with total charges avoids any nonlinear computational step and memory occupation. Furthermore, it also shows a good convergence for the C-PCM and IEF-PCM versions, which were quite problematic for the conventional separate charges approach. Also, first and second analytical derivatives are available in this context for Hartree–Fock and Kohn–Sham models. A number of examples are analyzed; they show that the new algorithms couple fully satisfactory numerical accuracy with remarkable computational efficiency. © 1999 John Wiley & Sons, Inc. J Comput Chem 20: 1186–1198, 1999

Keywords: polarizable continuum model; iterative procedures; large molecules in solution

Introduction

Theoretical and computational chemistry are presently facing the very demanding challenge of expanding the applicability of the quantum mechanical approaches to large molecules. Hardware and software developments are both contributing to this task, leading to the first applications of reliable electronic structure methods to macromolecular systems. A leading role in this progress is played by the use of fast multipole moment methods,[1] sparse matrix techniques, and conjugate gradient density matrix search techniques for solving the self-consistent field (SCF) problem.[2] Faster algorithms were developed for geometry optimizations of large molecules,[3] and

Correspondence to: Prof. V. Barone; e-mail: enzo@chemna.dichi.unina.it

CCC 0192-8651 / 99 / 111186-13

effective composite methods[4] further reduced computer times. In this context, the situation is particularly favorable for Hartree–Fock (HF) and Kohn–Sham (KS) methods but promising progress has been made for post-HF models, too. These developments call for analogous reformulation of models describing solvation effects: for the continuum solvent models in particular, a number of attempts toward linear scaling codes have been made for molecular mechanics[5] and semiempirical[6] techniques. However, until now much less effort has been expended to increase the performance of solvent models nested on *ab initio* methods for the treatment of macromolecules in condensed phases. A first step in this direction was provided by an updated iterative version[7] of the polarizable continuum model (PCM) in its original dielectric formulation (D-PCM)[8] that significantly improves its performances (memory and time scaling) without impairing the peculiar high accuracy of the results. In the present article we further improve the iterative model and extend it to all the variants of PCM [D-PCM,[8] conductor PCM (C-PCM),[9] integral equation formalism PCM (IEF-PCM[10])] for the effective computation of free energies and their analytical first and second derivatives with respect to geometrical parameters.

PCM is a self-consistent reaction field (SCRF) method in which the reaction field representing the electrostatic solute–solvent interactions is described by a finite set of polarization charges centered on small finite elements (tesserae) spread on the surface of a suitable molecular cavity surrounding the solute.

Because the number of tesserae increases linearly with the dimension of the solute, the steps that strongly depend on the size of the system in the PCM scheme are the construction of the cavity, the calculation of the electrostatic reaction potential, and the determination of the polarization charges.

In regard to the first point, the GEPOL procedure[11] traditionally used for building the solute cavity is remarkably fast and efficient for small and medium size molecules, especially in its more recent formulations employing the Gauss–Bonnet theorem,[12] an effective united atom topological model (UATM),[13] and a variable tesselation of the spheres.[14] For larger solutes the new DefPol procedure[15] is even more promising, but it has not been considered in the present work because for nonempirical quantum mechanical computations the other two limiting steps grow beyond reasonable computer resources far before the stage at which DefPol profitably replaces GEPOL. The calculation of the electrostatic reaction potential is closely related to that of the nuclear attraction energy of electrons (one-electron terms of the solute Hamiltonian), and its formulation can exploit the same low-scaling techniques developed for the electronic problem *in vacuo*.[1,2] The remaining bottleneck in a PCM calculation is the evaluation of the polarization charges, and this is precisely the topic on which the present work is focused. In the next section we show in detail the new procedure for determining apparent charges in the evaluation of free energies and their analytical first and second derivatives in solution at low cost and for all the PCM versions presently available in the Gaussian package.[16]

General Aspects of PCM

In the PCM procedure the solute molecule, possibly supplemented by some explicit solvent molecules belonging to the first solvation shell (e.g., as in ref. 17), is embedded in a cavity of molecular shape, which is surrounded by a polarizable continuum (dielectric or conductor) medium. The cavity is formed by interlocking spheres centered on solute atoms or atomic groups and its surface is partitioned into small elements called tesserae, which are obtained by projecting the faces of inscribed polyhedra on each sphere. By choosing a suitable polyhedron, one can define rougher or finer surface partitions as shown, for example, in Figure 1.

Each tessera i is characterized by its area a_i, its central point $\mathbf{r}_i$, and the unit vector normal to the cavity surface passing through the central point $\hat{n}_i$.

In this model the solute–solvent interactions are described in terms of the reaction field due to the polarization of the medium induced by the solute. The reaction field can be determined by solving the continuity equations

$$V_{\text{in}} = V_{\text{out}}, \tag{1}$$

$$\vec{\nabla} V_{\text{in}} \cdot \hat{n}_i = \varepsilon \vec{\nabla} V_{\text{out}} \cdot \hat{n}_i, \tag{2}$$

where V_{in} and V_{out} are the total (i.e., solute plus solvent) electrostatic potential at any point very close to the surface inside and outside the cavity, respectively, and ε is the dielectric constant of the external medium.

Systems (1) and (2) can be solved by placing on the cavity surface a polarization charge density σ

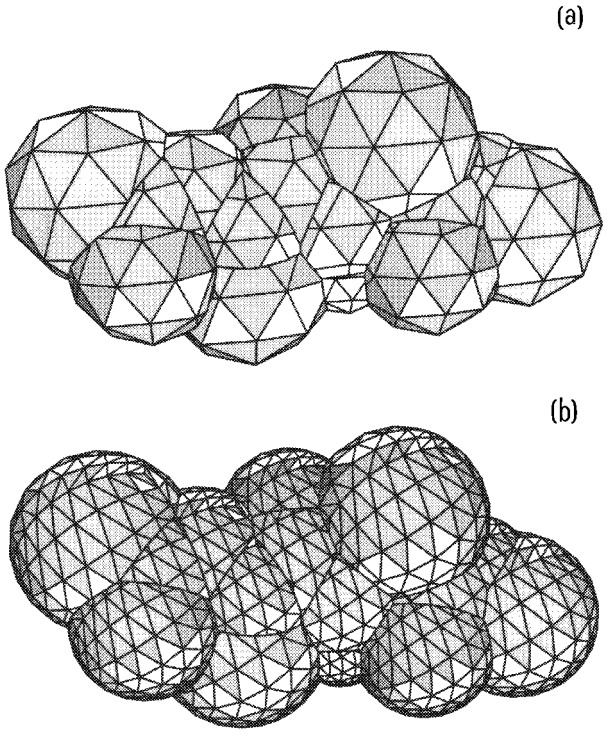

FIGURE 1. Molecular cavity generated by the standard GEPOL-UATM procedure for $Ace(Ala)_2NHMe$ by using (a) rougher or (b) finer surface partitions.

whose interaction with the solute is expressed by the operator $\hat{V}_\sigma$. In the computational practice σ is considered constant in each tessera, so that $\hat{V}_\sigma$ can be written in terms of a set of point charges:

$$\hat{V}_\sigma(\mathbf{r}) = \sum_i \frac{q_i}{|\mathbf{r} - \mathbf{r}_i|}. \tag{3}$$

Here and below index i on the summations runs over the number of cavity tesserae (Nt).

Then, if $\hat{H}^0$ is the Hamiltonian of the isolated solute, in the presence of the solvent the proper Hamiltonian operator becomes

$$\hat{H} = \hat{H}^0 + \hat{V}_\sigma. \tag{4}$$

Different algorithms, corresponding to slightly different physical models and mathematical approaches, have been proposed to determine the solvation charges q_i.[8–10]

They have the general expression

$$\mathbf{Dq} = -\mathbf{b}, \tag{5}$$

where the column vector $\mathbf{q}$ collects the solvation charges.

A detailed discussion of the peculiar characteristics and performance of each PCM variant is outside the purposes of the present study. We only recall that $\mathbf{D}$ is always a square matrix of dimensions equal to the number of tesserae, depending on ε and on the tesserae geometrical parameters: physically it represents the electrostatic interaction matrix between the polarization charges, particularly the following:

1. D-PCM: the matrix element D_{ij} contains the electrostatic field that q_i exerts on q_j, so that it depends on the inverse of the square modulus of the distance between the charges, $|\mathbf{r}_{ij}|^2$. The column matrix $\mathbf{b}$ collects the normal components of the solute electrostatic field on the tesserae.
2. C-PCM: D_{ij} contains the electrostatic potential between q_i and q_j charges, so that it is symmetric and depends on the inverse of the modulus of the distance $|\mathbf{r}_{ij}|$. The column matrix $\mathbf{b}$ collects the solute electrostatic potential on the tesserae.
3. IEF-PCM: the expression for D_{ij} is quite complex, depending on a combination of the potential and electrostatic field between charges. In the actual implementation of the isotropic version, $\mathbf{b}$ is the solute potential on the tesserae, otherwise (anisotropic and ionic versions) $\mathbf{b}$ contains solute potential and electrostatic fields on the tesserae.

In all cases the $\mathbf{D}$ matrix is not sparse. A detailed expression for $\mathbf{b}$ and $\mathbf{D}$ can be found, for instance, in refs. 8 and 18.

Calculation of Solvation Free Energies: Two Equivalent Formalisms

The formal problem of including the solvent perturbation in the SCF cycle can be tackled from two different points of view. On the one hand, one can explicitly consider the partial dependence of $\hat{V}_\sigma$ on the solute wave function. In this case the best approach is to define two different sets of solvation charges: $\mathbf{q}^N$, which depends on the solute nuclei, and $\mathbf{q}^e$, which depends on the solute electrons. This approach has been extensively explained elsewhere[18,19]; we simply recall that in such a model the apparent surface charges are obtained by solving two linear systems analogous to eq. (5) and that the SCF procedure directly leads

to the molecular free energy in solution. If Ψ is the wave function perturbed by the solvent, the free energy can be written as

$$G_{\mathrm{sol}} = \langle \Psi | \hat{H}^0 | \Psi \rangle + V_{NN} + \tfrac{1}{2} \sum_i (q_i^{\mathrm{N}} + q_i^{\mathrm{e}})(V_i^{\mathrm{N}} + V_i^{\mathrm{e}}), \quad (6)$$

where V_i^{N} and V_i^{e} are the electrostatic potentials generated by solute nuclei and electrons, respectively, and V_{NN} is the solute nuclear repulsion energy.

This 'separate charges' formalism has been adopted in all the recent PCM applications because it explicitly shows the direct dependence of the solute–solvent interactions on the electronic density, allowing the derivation of an analytical expression for the first and second derivatives of the solvation free energy.[20, 21]

On the other hand, the solvation charges can be viewed as 'external' perturbations whose value is recomputed at each SCF iteration: in this case the SCF calculation leads to the energy in solution

$$E_{\mathrm{sol}} = \langle \Psi | \hat{H}^0 | \Psi \rangle + V_{NN} + \sum_i q_i V_i. \quad (7)$$

To obtain the correct free energy in solution one has to subtract from the energy in eq. (7) the work spent to create the solvation charges themselves, which is exactly one-half of the interaction energy,[8] so that one again obtains

$$G_{\mathrm{sol}} = \langle \Psi | \hat{H}^0 | \Psi \rangle + V_{NN} + \tfrac{1}{2} \sum_i q_i V_i. \quad (8)$$

In an unrestricted finite basis approach, the elements of the Fock matrices for α and β electrons are perturbed by the solvent through

$$F_{\mu\nu}^{\alpha} = F_{\mu\nu}^{0\alpha} + \sum_i q_i V_{\mu\nu}^i, \quad (9a)$$

$$F_{\mu\nu}^{\beta} = F_{\mu\nu}^{0\beta} + \sum_i q_i V_{\mu\nu}^i, \quad (9b)$$

with

$$V_{\mu\nu}^i = -\langle \chi_\mu | \frac{1}{|\mathbf{r} - \mathbf{r}_i|} | \chi_\nu \rangle, \quad (10)$$

where χ_μ and χ_ν are atomic basis functions. By adopting a unified formalism using a generalized Fock matrix in the unrestricted form, eqs. (9a) and (9b) can be referred to the HF and KS approaches: for a closed shell system they reduce to a single Fock matrix.

From now on we call this latter approach 'total charges' formalism to distinguish it from the separate charges formalism cited above. We emphasize that the two approaches are formally equivalent; the main advantage in the use of the latter is related to the solution of the PCM electrostatic problem for large solutes, as we show in detail below.

First and Second Derivatives of Solvation Free Energy

As detailed elsewhere,[20] analytical first derivatives of the PCM free energy can be obtained by adding to the expressions used for isolated molecules terms like

$$\tfrac{1}{2} \sum_i (q_i V_i)^x, \quad (11)$$

where the superscript denotes differentiation with respect to the nuclear coordinate x. In all the previous PCM implementations eq. (11) was repeatedly used for the nuclear and the electronic sources of solvation charges and electrostatic potentials.

However, the PCM derivative algorithm can be transformed in order to use the total charges formalism. In this case

$$\left[\frac{1}{2} \sum_i q_i V_i \right]^x = \sum_i q_i (V_i)^x + Z^x,$$

$$Z^x = \begin{cases} -\sum_i q_i (\mathbf{E}_i \cdot \mathbf{r}_i^x) + \dfrac{1}{2} \sum_i (D_{ij})^x q_i q_j \\ \quad \text{C-PCM; IEF-PCM} \\ \dfrac{2\pi\varepsilon}{\varepsilon - 1} \sum_{i \in \Gamma} \dfrac{q_i^2}{a_i} U_i(x) \\ \quad \text{for all PCM variants.} \end{cases} \quad (12)$$

where D_{ij}^x is an element of the derivative matrix $\mathbf{D}^x$, $\mathbf{E}_i$ is the solute electric field acting on tessera i, and $U_i(x)$ is a function of the nuclear displacement related to cavity geometrical parameters.[10]

In the same way second derivatives of free energy in solution contain the following term explicitly dependent on the solvent:

$$\left[\tfrac{1}{2} \sum_i (q_i V_i)^x \right]^y = \sum_i q_i V_i^{x,y} - \sum_i D_{ij}^{-1} V_i^x V_j^y. \quad (13)$$

Furthermore, second derivatives always require density derivatives, which can be obtained by the coupled perturbed (CP) procedure. The Fock matrix derivative used in CP equations is also solvent dependent:

$$(F_{\mu\nu})^x = \left(F^0_{\mu\nu}\right)^x + \sum_i q_j \left(V^i_{\mu\nu}\right)^x - \sum_{ij} D^{-1}_{ij} (V_j)^x V^i_{\mu\nu}. \tag{14}$$

In the same equations another term involves the electronic charges q^e_i only: however, it can be put in a form that does not contain any explicit reference to the solvation charges:

$$- \sum_{ij} D^{-1}_{ij} \left(\sum_{\lambda\sigma} P^y_{\lambda\sigma} V^j_{\lambda\sigma} \right) V^i_{\mu\nu}, \tag{15}$$

where μ, ν, λ, and σ indicate the usual atomic basis functions and $P^y_{\lambda\sigma}$ is an element of the density matrix derivative. The corrections to be used in the second derivatives algorithm were obtained (in both the separate and total charges formalisms) in the hypothesis of a direct relationship between solvation charges and solute electrostatic potential, so that C-PCM and IEF-PCM variants only can be employed in these calculations.

Normalization of Polarization Charges

Any description of the solvent reaction field by a finite set of localized apparent charges introduces numerical errors with respect to the continuous charge distribution $\sigma(\mathbf{s})$ spread on the cavity surface. Furthermore, in quantum mechanical methods the additional polarization volume due to the solute wave function lying outside the cavity is not considered in the perturbative part of the solute Hamiltonian (1). It is well known that the errors induced by these approximations can be decisive for the accuracy of the results, so that effective procedures to correct the apparent charge values are crucial for all the continuum solvation models.[22]

An important measure of the errors due to the discretization and to the outlying electrons is provided by the Gauss theorem, which states that the exact solvation charge spread on the whole surface should be equal to $(\varepsilon - 1)/\varepsilon$ times the overall solute charge, where ε is the solvent dielectric constant. Then the simplest normalization procedure (hereafter N1) employs an additive correction in which the deviation from the Gauss law ΔQ is uniformly spread over the tesserae:

$$q^{\text{norm}}_i = q_i + \frac{a_i}{\sum_i a_i} \Delta Q, \tag{16}$$

where

$$\Delta Q = Q^{\text{th}}_{\text{pol}} - \sum_i q_i. \tag{17}$$

In a slightly more refined procedure (hereafter N3) the charge fraction added on each tessera is evaluated by weighting ΔQ with the solute electronic density calculated on the tessera itself [$\rho_{\text{solute}}(\mathbf{s}_i)$]:

$$q^{\text{norm}}_i = q_i + \frac{a_i \cdot \rho_{\text{solute}}(\mathbf{s}_i)}{\sum_i a_i \, \rho_{\text{solute}}(\mathbf{s}_i)} \Delta Q. \tag{18}$$

A last procedure (hereafter N4) finds its theoretical justification in the fact that the complete treatment of the electrostatic problem of a diffuse charge distribution in a continuum medium must explicitly consider the solute electronic charge distribution lying outside the cavity [$\rho_{\text{solute}}(\mathbf{r}^{\text{out}})$] as a further source of apparent charge.[23] In this case a further solute–solvent interaction operator is considered:

$$\hat{V} = \hat{V}^{\sigma} + \hat{V}^{\text{bulk}} = \frac{1}{2} \sum_i \frac{q_i}{|\mathbf{r} - \mathbf{r}_i|} + \frac{1}{2} \sum_i \frac{q^{\text{eff}}_i}{|\mathbf{r} - \mathbf{r}_i|}, \tag{19}$$

where $\mathbf{q}^{\text{eff}}$ is a set of apparent charges representing the reaction field due to the real outlying electronic density. Note that a further multiplicative normalization (N2) proposed for the separate charges formalism[22] cannot be extended to the total charge algorithm.

In Tables I and II we compare the performance of the different normalization procedures in the separate and total charges formalisms by reporting hydration free energies computed at the HF/6–31 + G**/D-PCM and C-PCM levels.[24] Because of the larger errors due to the outlying charge, most of the compounds we chose as 'sample' molecules are anions.

Note the complete equivalence between the separate and total charge formalisms when exploiting N3 and N4 compensations. Further, the results for the 'separated' N2 and 'total' N1 procedures are quite close: the most important discrepancy occurs for the negatively charged and asymmetrical systems using D-PCM (2.04 kcal/mol for CH_3COO^- and 3.36 kcal/mol for CH_3O^-). However, we can conclude that the uniform distribution of the total

TABLE I.
Solvation Free Energies (kcal/mol) Calculated at HF/D-PCM Level Using Different Procedures for Normalization of Solvation Charges.

	Separate Charges Formalism			Total Charges Formalism		
	N2	N3	N4	N1	N3	N4
NH_2^- [a]	−95.80	−94.50	−93.21	−96.50	−94.51	−93.22
PH_2^- [a]	−66.98	−66.41	−65.89	−67.15	−66.41	−65.88
OH^- [a]	−111.56	−109.63	−108.08	−112.09	−109.63	−108.05
SH^- [a]	−74.39	−73.63	−73.00	−74.53	−73.63	−72.98
F^- [a]	−107.02	−107.02	−107.02	−107.02	−107.02	−107.02
CH_3COO^- [a]	74.53	−76.61	−78.08	−72.49	−76.53	−78.00
CH_3O^- [a]	−88.19	−91.36	−94.28	−84.83	−91.32	−94.25
H_3O^+ [b]	−105.79	−105.50	−105.29	−105.83	−105.50	−105.32
CH_4 [b]	1.83	1.85	1.86	1.83	1.85	1.86
CH_3OH [b]	−5.31	−5.07	−4.97	−5.26	−5.05	−5.02
NH_3 [b]	−4.60	−4.44	−4.33	−4.64	−4.44	−4.33
CH_3COH [b]	−3.96	−3.68	−3.60	−3.85	−3.65	−3.63

[a] 6–31 + G* basis set.
[b] 6–31G* basis set.

error by using constant multiplicative factors (separate N2) or by using additive weighted corrections (total N1) are practically equivalent in most cases.

Effective Iterative Algorithm

The charges q_i are found by solving the electrostatic problem of charged particles (solute nuclei and electrons) in a cavity dug in the polarizable medium.

Although the first implementations of PCM used iterative algorithms to solve the system, the quest for more accurate solutions and for energy gradients led to the introduction of a different strategy in which the **D** matrix is inverted during the first SCF cycle and $\mathbf{D}^{-1}$ is stored for later use (for both further SCF cycles and evaluation of energy gradients).

The solution of the PCM electrostatic problem is the most time consuming step in the calculation for large solutes: it coincides with the more general problem of the evaluation of *N*-body electro-

TABLE II.
Solvation Free Energies (kcal/mol) Calculated at HF/C-PCM Level Using Different Procedures for Normalization of Solvation Charges.

	Separate Charges Formalism		Total Charges Formalism	
	N2	N3	N1	N3
NH_2^- [a]	−95.49	−95.24	−95.73	−95.26
PH_2^- [a]	−66.83	−66.74	−66.86	−66.74
OH^- [a]	−111.00	−110.68	−110.98	−110.68
SH^- [a]	−74.05	−73.93	−74.07	−73.93
F^- [a]	−107.02	−107.02	−107.02	−107.02
CH_3COO^- [a]	−77.25	−77.43	−77.06	−77.43
CH_3O^- [a]	−92.44	−92.81	−92.00	−92.81
H_3O^+ [b]	−105.11	−105.09	−105.11	−105.09
CH_4 [b]	1.86	1.86	1.86	1.86
CH_3OH [b]	−5.05	−5.03	−5.04	−5.03
NH_3 [b]	−4.32	−4.31	−4.33	−4.31
CH_3COH [b]	−3.54	−3.51	−3.53	−3.51

[a] 6–31 + G* basis set.
[b] 6–31G* basis set.

static interactions, which has motivated much theoretical work during the last few years. The time request for the matrix inversion algorithm grows with an Nt^3 scaling and the memory occupation grows as Nt^2, where Nt is the number of tesserae. This is the main reason why PCM calculations have not yet been considered for very large molecules.

An alternative to the explicit solution through inversion of **D** was recently implemented for D-PCM within the traditional separate charges formalism.[7] We extended the same basic idea to all the PCM variants considering a total charges implementation of the algorithm.

Let us consider the explicit expression for the surface charge i:

$$q_i = \frac{-b_i}{D_{ii}} - \frac{1}{D_{ii}} \sum_{j \neq i} D_{ij} q_j, \tag{20}$$

where b_i is the solute electric field or the potential, depending on the model to which we are referring. As a first approximation we consider that the q_i is obtained by neglecting the second term in the right-hand side of eq. (20):

$$q_i^{(0)} = \frac{-b_i}{D_{ii}}. \tag{21a}$$

Then we have

$$q_i^{(n)} = q_i^{(0)} - \frac{1}{D_{ii}} \sum_{j \neq i} D_{ij} \cdot q^{(n-1)}. \tag{21b}$$

In regard to memory occupation the algorithm was implemented in the following way:

1. D-PCM and C-PCM: the code does not involve any memory allocation for the **D** matrix because its elements are simple enough to be recomputed at each iteration.
2. IEF-PCM: the **D** matrix is stored on external devices and only one column is transferred in the core for each step of the algorithm.

In all the cases the storage of the two vectors $\mathbf{q}^0$ and $\mathbf{q}^{n-1}$ is required.

Convergence within Nt iterations in guaranteed if **D** is diagonally dominant: this condition is generally satisfied by D-PCM because in this case, although **D** is not sparse, its off-diagonal elements inversely depend on the squared modulus of $\mathbf{r}_{ij}$. The situation is less favorable for models depending on the solute electrostatic potential, because in this case the off-diagonal **D** elements depend on the inverse of $|\mathbf{r}_{ij}|$. The main advantage in using the total charges formalism lies in the fact that the convergence speed of the iterative procedure just described increases markedly, especially for the C-PCM and IEF-PCM approaches. This is what one could expect, noting that on each tessera the total apparent charge is smaller in absolute value than the nuclear and electronic contribution, respectively, because of the partial compensation of the two opposite effects. As a consequence, the sum in eq. (21b) is also smaller than using the separate charges formalism, leading to a faster convergence even for the less favorable models. We can see this in more detail by defining the error with respect to the solution **q** at the nth iteration as

$$\mathbf{e}^{(n)} = \mathbf{q}^{(n)} - \mathbf{q}. \tag{22}$$

At the zeroth iteration we can write

$$\begin{aligned} \mathbf{e}^{(0)} &= \mathbf{q}^{(0)} - \mathbf{q} = (\mathbf{q}^{\mathrm{N}(0)} - \mathbf{q}^{\mathrm{N}}) + (\mathbf{q}^{\mathrm{e}(0)} - \mathbf{q}^{\mathrm{e}}) \\ &= \mathbf{e}^{\mathrm{N}(0)} + \mathbf{e}^{\mathrm{e}(0)}, \end{aligned} \tag{23}$$

where the superscripts N and e refer to the nuclear and electronic contributions, respectively, in the separated charges approach. At this point we must consider the peculiar characteristic of systems (21a) and (21b): first, the zeroth-order approximations for q_i^{N} and q_i^{e} [eq. (21a)] have a definite and correct sign (positive for the charges induced by electrons and negative for those induced by nuclei). Second, $|q_i^{(0)}|$ is an upper bound to $|q_i|$, so we can write

$$\begin{aligned} \mathbf{e}^{\mathrm{N}(0)} &< 0, \\ \mathbf{e}^{\mathrm{e}(0)} &> 0 \end{aligned} \tag{24}$$

from this inequality and from eq. (23) we can write

$$\|\mathbf{e}^{(0)}\|_1 < \|\mathbf{e}^{\mathrm{N}(0)}\|_1 + \|\mathbf{e}^{\mathrm{e}(0)}\|_1, \tag{25}$$

where $\|\mathbf{e}\|_1 = \Sigma_i |e_i|$. This partial compensation of the two errors since the zeroth iteration definitely leads to a faster convergence with respect to the separate solution of system (5). At the nth iteration we therefore have the inequality

$$\|\mathbf{e}^{(n)}\|_1 < \|\mathbf{e}^{\mathrm{N}(n)}\|_1 + \|\mathbf{e}^{\mathrm{e}(n)}\|_1 \quad n > 0. \tag{26}$$

An even better behavior can be achieved by taking into account the following aspects.

In eq. (21) $|q_i^{(0)}|$ is an upper bound to $|q_i|$, so that the second term on the right-hand side of eq. (21b) is overestimated in the first iteration and determines an underestimated value for $q_i^{(1)}$. Then in

the second iteration the second term on the right-hand side of eq. (21b) is underestimated, leading to an overestimated value for $q_i^{(2)}$, and so on. We obtain a damped oscillating behavior in which the residual

$$\delta_i^{(n)} = q_i^{(n)} - q_i^{(n-1)} \tag{27}$$

decreases in absolute value and generally satisfies the condition

$$\frac{\delta_i^{(n)}}{\delta_i^{(n-1)}} < 0. \tag{28}$$

Then a test in the sign of the largest residual is performed at each two iterations and improved values of polarization charges are obtained by a balanced two-term interpolation

$$q_i = \lambda q_i^{(n)} + (1 - \lambda) q_i^{(n-1)} \tag{29}$$

with

$$\lambda = \frac{|1/\delta_M^{(n)}|}{|1/\delta_M^{(n)}| + |1/\delta_M^{(n-1)}|} \tag{30}$$

if condition (28) is satisfied and $\lambda = 1$ otherwise; in eq. (30) the $\delta_M^{(n)}$ is the largest residual at the nth iteration and its absolute value is also used as a convergence criterion.

In order to show the behavior of the iterative procedure, Figures 2 and 3 show an example of the typical trend of δ_M with respect to the number of iterations obtained using different formalisms.

Note that by using an interpolated total charges formalism the number of iterations is reduced by a factor of 5 in the D-PCM case for each SCF cycle and that in C-PCM the application of this procedure also notably improves the convergence speed. Analogous results were obtained for the isotropic, anisotropic, and ionic IEF-PCM procedures.

The effectiveness of the method is related, of course, to the convergence threshold. A number of test calculations showed that a value of 10^{-6} is sufficient to give a comparable accuracy of the calculated energy with respect to the traditional separated charges matrix inversion procedure. Moreover, the tests showed a further improvement in the saving time using the value of 10^{-4} for the threshold during the first SCF step and then halved values at each SCF step until the limit of 10^{-6} was reached. A similar technique was applied for the electronic charges $\mathbf{q}^e$ in the separated charges formalism,[23] which converged the nuclear charges $\mathbf{q}^N$ to 10^{-6} at the beginning of the computation however.

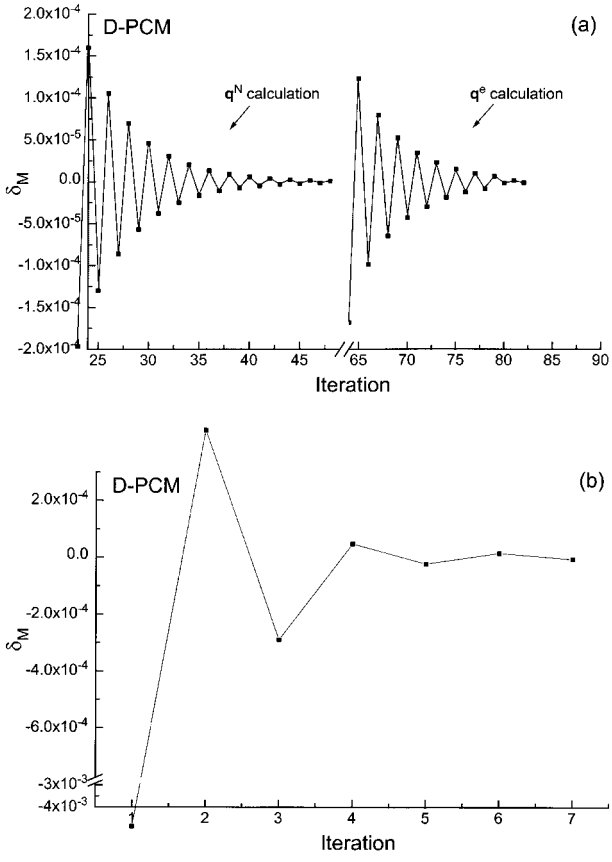

FIGURE 2. Convergence of polarization charges for D-PCM computations: (a) separated charges formalism without interpolation and (b) total charges formalism with interpolation.

The interpolated total charges formalism was implemented in the development version of the Gaussian program[16] for all the PCM procedures to perform free energies calculations and geometry optimizations in solution. Note that these are possible because by exploiting eq. (12) in calculating the free energy gradients the use of the **D** matrix is no longer necessary.

Numerical Results

We now present some numerical results to compare the performance of the procedures now available for PCM calculations. A first sample was formed by small and medium size molecules for which we compared the accuracy and the efficiency of all the PCM variants. Next we considered the model peptides $CH_3CO—(NH—CHCH_3—CO)_n—NHCH_3$ with n going from 1 to 11 [hereafter Ace(Ala)$_n$NHMe)] involving a number

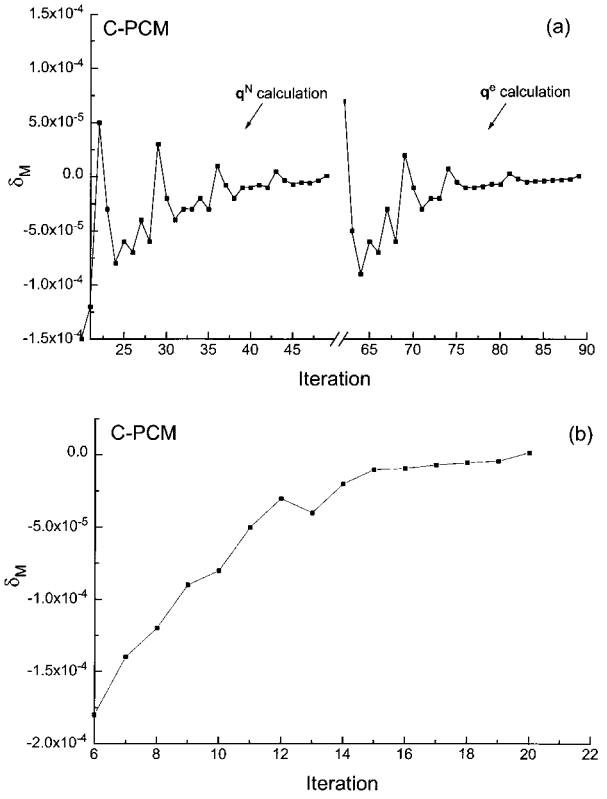

FIGURE 3. Convergence of polarization charges for C-PCM computations: (a) separated charges formalism with interpolation and (b) total charges formalism with interpolation.

of tesserae (Nt) up to 3600 to show the high performance of the total iterative technique with respect to the traditional one.

In all the cases the cavities were built according to the GEPOL-UATM model.[13] All the geometries were obtained by full optimizations at the HF/6–31G* level,[24] except for the peptides, whose β-sheet conformations were fully optimized by the AMBER force field.[25] Finally all the test calculations were done at the HF level using the 6–31G* basis set in the neutral compounds and the 6–31 + G* basis set in the anions.

We report in Table III the results obtained by the separate and total charges formalisms and the matrix inversion and iterative procedures at the D-PCM level. Tables IV and V refer to the analogous results obtained at the C-PCM and isotropic IEF-PCM levels, respectively. In the tables the free hydration energies and the CPU time involved by the PCM routines (on an IBM R6K/3CT workstation) are shown. The number of iterations in which the convergence was reached in the iterative procedures is also reported: they refer to the first SCF step during which the same threshold of 10^{-6} was adopted for nuclear, electronic, and total charges with the aim of comparing the different algorithms in a unbiased way.

In regard to the D-PCM calculations, note first the same free energy values obtained by exploiting

TABLE III.
Solvation Free Energies (kcal/mol) Calculated at HF/6–31G*/D-PCM Level Using Different Algorithms.

		Separate Charges Formalism					Total Charges Formalism				
		Matrix Inversion		Iterative			Matrix Inversion		Iterative		
	No. Tesserae	ΔG_{solv}	CPU Time	ΔG_{solv}	CPU Time	No. Iter.	ΔG_{solv}	CPU Time	ΔG_{solv}	CPU Time	No. Iter.
H_2O	118	−8.37	8.8	−8.37	7.1	18	−8.31	6.9	−8.31	6.9	7
NH_3	145	−5.67	10.2	−5.67	8.0	18	−5.63	7.8	−5.63	7.6	6
CH_4	196	1.45	10.8	1.45	6.4	16	1.45	7.0	1.45	6.0	7
CH_3OH	233	−4.80	20.5	−4.80	14.6	20	−4.70	14.7	−4.70	13.6	8
NH_2CH_3	256	−3.23	24.8	−3.23	17.1	28	−3.15	17.4	−3.15	15.5	9
CH_3COOH	300	−7.59	50.0	−7.59	37.8	28	−7.44	37.8	−7.44	35.6	8
C_2H_6	308	2.54	27.2	2.54	13.4	17	2.55	16.7	2.55	11.7	6
$N(CH_3)_3$	509	2.28	115.6	2.28	61.0	27	2.33	74.8	2.33	54.5	7
CH_3O^- [a]	206	−90.18	20.6	−90.18	18.9	66	−90.11	15.8	−90.11	16.0	29
CH_3COO^- [a]	295	−81.18	55.9	−81.18	43.5	25	−80.90	43.4	−80.90	41.6	8
Ace(Ala)NMe	681	−17.72	374.0	−17.72	354.	31	−17.54	373.1	−17.54	304.8	17
$Ace(Ala)_2NMe$	955	−23.73	915.3	−23.73	823.6	35	−22.81	915.0	−22.81	687.3	19

The number of iterations involved in the first SCF cycle and the total CPU times are also reported.
[a] 6–31 + G* basis set.

TABLE IV.
Solvation Free Energies (kcal/mol) Calculated at HF/6–31G*/C-PCM Level Using Different Algorithms.

		Separate Charges Formalism					Total Charges Formalism				
		Matrix Inversion		Iterative			Matrix Inversion		Iterative		
	No. Tesserae	ΔG_{solv}	CPU Time	ΔG_{solv}	CPU Time	No. Iter.	ΔG_{solv}	CPU Time	ΔG_{solv}	CPU Time	No. Iter.
H_2O	118	−8.40	8.2		NC		−8.40	6.5	−8.41	6.6	28
NH_3	145	−5.66	9.4	−5.66	9.8	68	−5.65	7.2	−5.65	7.4	19
CH_4	196	1.49	10.0	1.51	7.8	66	1.49	6.4	1.50	5.3	8
CH_3OH	233	−4.74	17.1	−4.73	18.7	115	−4.74	12.0	−4.73	12.3	27
NH_2CH_3	256	−3.16	20.6		NC		−3.16	14.1	−3.16	15.6	24
CH_3COOH	300	−7.42	34.4	−7.42	40.0	180	−7.42	24.7	−7.42	27.1	30
C_2H_6	308	2.57	23.5	2.58	23.3	143	2.57	14.1	2.57	9.3	8
$N(CH_3)_3$	509	2.51	91.0	2.51	73.3	108	2.52	55.6	2.52	34.2	20
CH_3O^- [a]	206	−89.45	16.2	−88.86	18.3	152	−89.53	12.3	−89.52	12.7	26
CH_3COO^- [a]	295	−80.25	35.3	−80.32	34.1	117	−80.31	26.1	−80.31	26.8	37
Ace(Ala)NMe	681	−18.32	187.3	−18.32	242.0	193	−18.31	186.4	−18.31	171.3	48
$Ace(Ala)_2NMe$	955	−24.97	511.26		NC		−24.83	510.7	−24.82	419.9	52

The number of iterations involved in the first SCF cycle and the total CPU times are also reported. NC, not converged.
[a] 6–31+G* basis set.

the matrix inversion and the iterative procedures: the small differences we observe comparing both formalisms are due to the different normalization procedures. Then consider the first and the third columns in Table III (i.e., compare the matrix inversion and the iterative version exploiting the separated charges formalism): note that we have a notable saving in CPU time (the average value is 26%), even if quite small compounds are considered. Comparing the results obtained by exploiting the total charges formalism, the iterative method affords an average time savings of 32% with respect to the traditional separate inversion method and it becomes competitive with regard to the corresponding inversion or the separate iterative method increasing the solute size; note however

TABLE V.
Solvation Free Energies (kcal/mol) Calculated at HF/6–31G*/IEF-PCM Level Using Different Algorithms.

		Separate Charges Formalism					Total Charges Formalism				
		Matrix Inversion		Iterative			Matrix Inversion		Iterative		
	No. Tesserae	ΔG_{solv}	CPU Time	ΔG_{solv}	CPU Time	No. Iter.	ΔG_{solv}	CPU Time	ΔG_{solv}	CPU Time	No. Iter.
H_2O	118	−8.33	6.9		NC		−8.34	6.9	−8.35	8.2	31
NH_3	145	−5.61	8.0	−5.61	9.7	80	−5.60	8.0	−5.60	7.8	30
CH_4	196	1.50	8.3	1.50	9.0	77	1.50	8.3	1.50	6.4	9
CH_3OH	233	−4.67	15.1		NC		−4.69	15.1	−4.68	12.8	26
CH_3O^- [a]	206	−88.46	14.5		NC		−89.43	14.5	−89.43	13.5	38
NH_2CH_3	256	−3.11	25.5		NC		−3.12	25.5	−3.12	20.5	30
$N(CH_3)_3$	509	2.54	88.7	2.55	70.6	155	2.54	88.7	2.56	46.0	29
CH_3COOH	300	−7.37	31.3	−7.37	32.3	188	−7.36	31.3	−7.36	26.2	36
CH_3COO^- [a]	295	−80.22	32.4	−78.94	29.8	100	−80.21	32.4	−80.21	28.0	79
C_2H_6	308	2.57	21.2	2.57	19.6	188	2.57	21.2	2.57	13.7	52
Ace(Ala)NMe	681	−18.29	472.7		NC		−18.14	471.1	−18.14	318.3	73
$Ace(Ala)_2NMe$	955	−25.47	1632.0		NC		−24.54	1631.5	−24.50	1059.2	76

The number of iterations involved in the first SCF cycle and the total CPU times are also reported. NC, not converged.
[a] 6–31+G* basis set.

the lower number of iterations in which the convergence is reached in the total charges approach. Furthermore, it is interesting to observe that for small compounds (Nt up to 500) the total charges procedure involves a notable savings of computer time with respect to the separated charges version, even when the matrix inversion is considered. This behavior is no longer retained when increasing the solute size. Finally, we can say that in the D-PCM case the performance of all the procedures available are comparable in the small compounds, while the efficiency of the total iterative method becomes very competitive in increasing the solute size.

Let us now consider the results obtained by exploiting the methods dependent on the electrostatic potential (C-PCM and IEF-PCM): also, in this case we have the same accuracy in calculating free solvation energies by exploiting the inversion and iterative methods, the largest differences being due to the normalization procedures used according to the separated or total formalism adopted. Once again the total charges matrix inversion algorithm is already less computer intensive than its separate charge counterpart for small solutes. Note, however, that the separate iterative method does not converge in some cases and always involves a huge number of iterations. On the contrary, the total iterative algorithm appears stable and more efficient: the saved time amounts to 17.9% for C-PCM and 35% for IEF-PCM with respect to the traditional procedure. So we can conclude that in the C-PCM and IEF-PCM versions only the inversion procedure can be safely used when exploiting the separated charges formalism, whereas the iterative method becomes competitive using the total charges formalism.

In Figure 4 the percent savings in CPU time of the total iterative procedure with respect to the traditional matrix inversion separate procedure is shown versus the number of tesserae: the results refer to the D-PCM and C-PCM free energy calculations of Ace(Ala)$_n$NHMe peptides. The larger compound involves 11 residues and 3596 tesserae. Note that the savings in computer time increases significantly and reaches a value of 79% for the D-PCM and 68% for the C-PCM. The method is also quite stable: a progressive reduction of the threshold in successive SCF cycles led to an average number of iterations per SCF cycle that was lower than 15 in the D-PCM and lower than 25 in the C-PCM.

As a last point, we show that the new formalisms can also be used for geometry optimizations and harmonic frequency computations. A

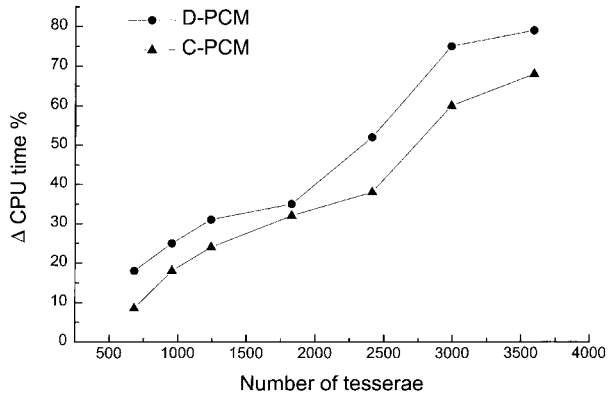

FIGURE 4. Percent savings in CPU time of the total iterative procedure with respect to the matrix inversion separate procedure for D-PCM and C-PCM free energy calculations of Ace(Ala)$_n$NHMe.

number of tests showed that the results obtained by the different algorithms are virtually indistinguishable and that the convergence thresholds used in the SCF procedure are also sufficiently accurate in the computation of energy derivatives. For purposes of comparison, Table VI reports the geometries computed *in vacuo* and in aqueous solution (D-PCM iterative version with total charges) at the HF/6−31G* level for acetic acid and acetamide (Fig. 5) and the corresponding computer times.

These results confirm that the new algorithms already give reliable results in reasonable computer times for small solutes, and the situation improves significantly for large systems.

Conclusion

In this article we introduced and validated some new procedures that improve the performance of the PCM and extend its field of application to larger solutes. All the different variants of PCM benefit from the new implementation and, in particular, iterative C-PCM and IEF-PCM are now feasible for large systems due to the total charges formalism. Also, analytical first and second derivatives remain available for HF and KS methods

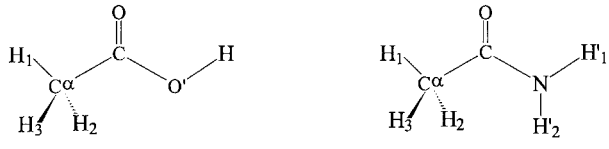

FIGURE 5. Schematic drawing and atom numbering for acetic acid and acetamide.

TABLE VI.

Geometrical Parameters (Å and degrees) Obtained at HF/6–31G*/D-PCM Level for Acetic Acid and Acetamide.

	CH_3COOH		CH_3CONH_2	
	Vacuum	Aq. Sol.	Vacuum	Aq. Sol.
CC^{α}	1.502	1.499	1.512	1.510
CO	1.190	1.194	1.208	1.212
CO′	1.334	1.322		
CN			1.354	1.340
$C^{\alpha}CO$	125.48	125.26	122.45	122.30
$C^{\alpha}CO'$	112.14			
$C^{\alpha}CN$			115.63	115.23
$CC^{\alpha}H_1$	109.96	109.96	109.44	109.44
$CC^{\alpha}H_2$	109.71	109.57	110.33	110.33
$CC^{\alpha}H_3$	109.71	109.57	110.33	110.33
CO′H	110.23	109.91		
CNH'_1			120.92	120.83
CNH'_2			120.92	120.83
$OCC^{\alpha}H_1$	0.00	0.00	0.00	0.00
$OCC^{\alpha}H_2$	120.98	120.98	120.45	120.46
$OCC^{\alpha}H_3$	120.98	120.98	239.47	239.47
$O'CC^{\alpha}H_1$	180.00	180.00		
$NCC^{\alpha}H_1$			180.00	180.00
$C^{\alpha}CO'H$	180.00	180.00		
$C^{\alpha}CNH'_1$			180.00	180.00
$C^{\alpha}CNH'_2$			0.00	0.00
t_{PCM}/t_{vac}		1.22		1.24

See Figure 5 for atom numbering and main text for details.

with time and memory requests that are improved (gradients) or comparable (Hessians) to previous versions. Coupling of these new procedures with other algorithmic improvements (e.g., proper treatment of symmetry[26]) further enhances the performance of PCM, which is now comparable to those of computations *in vacuo* concerning time and memory occupation for energies and geometry optimizations.

References

1. (a) Greengard, L.; Rokhlin, V. J Comput Phys 1987, 73, 325; (b) Greengard, L. The Rapid Evaluation of Potential Fields in Particle Systems; MIT Press: Cambridge, MA, 1998; (c) Greengard, L. Science 1998, 265; (d) White, C. A.; Head–Gordon, M. J Chem Phys 1994, 101, 6593; (e) Burant, M. C.; Strain, G.; Scuseria, G. E.; Frisch, M. J. Chem Phys Lett 1996, 248, 43; (f) Strain, M. C.; Scuseria, G. E.; Frisch, M. J. Science 1996, 271, 51.
2. (a) Millam, J. M.; Scuseria, E. G. J Chem Phys 1997, 106, 5569; (b) Daniels, A. D.; Millam, J. M.; Scuseria, G. E. J Chem Phys 1997, 107, 425.
3. Farkas, O.; Schlegel, H. B. J Chem Phys 1998, 109, 7100.
4. (a) Maseras, F.; Morokuma, K. J Comput Chem 1995, 16, 1170; (b) Dapprich, S.; Komaromi, I.; Bynn, K. S.; Morokuma, K.; Frisch, M. J. Theor Chem Acc to appear.
5. (a) Bharadwaj, R.; Windemuth, A.; Sridharau, S.; Honig, B.; Nicholls, A. J Comput Chem 1995, 16, 898; (b) Zanhar, R. J.; Varnek, A. J Comput Chem 1996, 17, 864; (c) Vorobjev, Y. N.; Scheraga, H. A. J Comput Chem 1997, 18, 569; (d) Purisima, E. O. J Comput Chem 1998, 13, 1494.
6. York, D. M.; Lee, T. S.; Yang, W. Chem Phys Lett 1996, 263, 297.
7. Rega, N.; Cossi, M.; Barone, V. Chem Phys Lett 1998, 293, 221.
8. (a) Miertus, S.; Scrocco, E.; Tomasi, J. Chem Phys 1981, 55, 117; (b) Amovilli, C.; Barone, V.; Cammi, R.; Cances, E.; Cossi, M.; Mennucci, B.; Pomelli, C.; Tomasi, J. Adv Quantum Chem 1998, 32, 227.
9. Barone, V.; Cossi, M. J Phys Chem A 1998, 102, 1995.
10. Cancès, E.; Mennucci, B.; Tomasi, J. J Chem Phys 1997, 107, 3032.
11. Pascual–Ahuir, J. L.; Silla, E.; Tomasi, J.; Bonaccorsi, R. J Comput Chem 1987, 8, 778.
12. Cossi, M.; Mennucci, B.; Cammi, R. J Comput Chem 1996, 17, 56.
13. Barone, V.; Cossi, M.; Tomasi, J. J Chem Phys 1997, 107, 3210.
14. Pomelli, C. S.; Tomasi, J. Theor Chem Acc 1998, 99, 34.
15. Pomelli, C. S.; Tomasi, J. J Comput Chem 1998, 19, 1758.

16. Frisch, M. J.; Trucks, G. W.; Schlegel, H. B.; Scuseria, G. E.; Robb, M. A.; Cheeseman, J. R.; Zakrzewski, V. G.; Montgomery, J. A.; Stratmann, R. E.; Burant, J. C.; Dapprich, S.; Millam, J. M.; Daniels, A. D.; Kudin, K. N.; Strain, M. C.; Farkas, O.; Tomasi, J.; Barone, V.; Cossi, M.; Cammi, R.; Mennucci, B.; Pomelli, C.; Adamo, C.; Clifford, S.; Ochterski, J.; Petersson, G. A.; Ayala, P. Y.; Cui, Q.; Morokuma, K.; Malick, D. K.; Rabuck, A. D.; Raghavachari, K.; Foresman, J. B.; Cioslowski, J.; Ortiz, J. V.; Stefanov, B. B.; Liu, G.; Liashenko, A.; Piskorz, P.; Komaromi, I.; Gomperts, R.; Martin, R. L.; Fox, D. J.; Keith, T.; Al-Laham, M. A.; Peng, C. Y.; Nanayakkara, A.; Gonzalez, C.; Challacombe, M.; Gill, P. M. W.; Johnson, B.; Chen, W.; Wong, M. W.; Andres, J. L.; Head–Gordon, M.; Replogle, E. S.; Pople, J. A. Gaussian 99, Development Version (Revision A.6); Gaussian, Inc.: Pittsburgh, PA, 1998.
17. Rega, N.; Cossi, M.; Barone, V. J Am Chem Soc 1998, 120, 5723.
18. Cammi, R.; Tomasi, J. J Comput Chem 1995, 16, 1449.
19. Hoshi, H.; Sakurai, M.; Inoue, Y.; Chujo, R. J Chem Phys 1987, 87, 1107.
20. Cossi, M.; Barone, V. J Chem Phys 1998, 109, 6246.
21. Cammi, R.; Tomasi, J. J Chem Phys 1994, 101, 3888.
22. (a) Klamt, A.; Jonas, V. J Chem Phys 1996, 105, 9972; (b) Baltrige, K.; Klamt, A. J Chem Phys 1997, 106, 6622; (c) Chipman, D. M. J Chem Phys 1996, 104, 3276; (d) Chipman, D. M. J Chem Phys 1997, 106, 10194.
23. Mennucci, B.; Tomasi, J. J Chem Phys 1997, 106, 5151.
24. Foresman, J. B.; Frisch, A. E. Exploring Chemistry with Electronic Structure Methods, 2nd ed.; Gaussian, Inc.: Pittsburgh, PA, 1996.
25. Cornell, W. D.; Cieplak, P.; Bayly, C. I.; Gould, I. R.; Merz, K. M., Jr.; Ferguson, D. M.; Spellmeyer, D. C.; Fox, T.; Caldwell, J. W.; Kollman, P. A. J Am Chem Soc 1995, 117, 5179.
26. Scalmani, G.; Barone, V. Chem Phys Lett 1999, 301, 263.